Published in : Journal of Applied Polymer Science (2021), vol. 138, n°21, e 50769
DOI: 10.1002/app.50769
Status : Postprint (Author's version)

PHOTOACTIVE MUSSELS INSPIRED POLYMER COATINGS: PREPARATION AND ANTIBACTERIAL ACTIVITY

Rayna Bryaskova[1], Nikoleta Philipova[1], Nikolay Georgiev[2], Ivo Lalov[3], Vladimir Bojinov[2], Christophe Detrembleur[4]

[1] *Department of Polymer Engineering, University of Chemical Technology and Metallurgy, Sofia, Bulgaria*
[2] *Department of Organic Synthesis, University of Chemical Technology and Metallurgy, Sofia, Bulgaria*
[3] *Department of Biotechnology, University of Chemical Technology and Metallurgy, Sofia, Bulgaria*
[4] *Center for Education and Research on Macromolecules (CERM), CESAM Research Unit, Chemistry Department, University of Liege, Liège, Belgium*

Correspondence : Rayna Bryaskova, Department of Polymer Engineering, University of Chemical Technology and Metallurgy, 8 Kliment Ohridsky Str., 1756 Sofia, Bulgaria. Email: rbryaskova@uctm.edu

Funding information
Bulgarian National Science Fund, Grant/Award Number: project no. KP-06-H29/5

ABSTRACT

In this article we report on the facile preparation of photoactive antibacterial mussel inspired polymer coatings deposited on a stainless steel (SS) substrate from water based precursors. The coating is prepared by the sequential deposition of aqueous based solutions of an anchoring layer based on bio-inspired glue, a cationic polymer bearing pendent catechols, a nanogel decorated by ortho-quinones and a photosensitizer of the aminoacridine type. This latter is grafted to the coating by reaction of its amino group with the o-quinone of the deposited nanogel. The deposition of all layers is followed in-line by Quartz crystal microbalance coupled with dissipation (QCM-D) and AFM shows that the thin polymer film repeated the roughness of the SS substrate. The prepared coatings show good mechanical properties applying nanoindentation techniques. The established antibacterial activity of the prepared photoactive polymer coatings on SS against Gram-negative E. coli strain demonstrate their potential as a power tool for medical applications

KEYWORDS : ADHESIVES, BIOMEDICAL APPLICATIONS, BIOMIMETIC, COATINGS, GRAFTING

Published in : Journal of Applied Polymer Science (2021), vol. 138, n°21, e 50769
DOI: 10.1002/app.50769
Status : Postprint (Author's version)

1. Introduction

Adhesion of various pathogens to different types of surfaces is one of the main causes of bacterial contamination. This requires the development of different strategies to prepare antibacterial coatings that will prevent the development of nosocomial infections, which are a topical and serious societal problems. Researcher's efforts are directed toward the design of surfaces that will suppress biofilm formation either by killing bacteria and/or by preventing their adhesion to surfaces. Control of bacterial growth can essentially be accomplished using three different strategies: (1) the use of "no-touch" methods as ultraviolet (UV) light[1–2] or aerolized and/or vaporized hydrogen peroxide;[3] (2) the use of super hydrophobic coatings that prevent bacterial adhesion to the substrates[4] and (3) the use of coatings that kill bacteria upon contact, where disintegration of the cell bacterial membrane occurs in contact with the coated substrate.[5–14] Many of these techniques consist in surface modification of the coatings by introducing antibacterial substances such as antibiotics, metals, antiseptics and various techniques such as adsorption, covalent binding or ligand-receptor interactions are applied.

In recent years, significant actuality gains to the so called "self-disinfecting" surfaces or "self-hygienic" surfaces which can lead to considerably reducing the frequency and level of surface contamination. Selfdisinfecting surfaces can be created by impregnation or by coating the surfaces with heavy metal ions (silver or copper), germicides (triclosan), or miscellaneous methods (e.g., light-activated antimicrobials). These methods are under active investigation but to date they have not been assessed for their ability to reduce health care-associated infections.[5]

The surfaces that release antibacterial compounds are effective, although ultimately they can be exhausted. Moreover, the use of antibacterial agents presents a potential problem due to the possibility of favoring bacterial resistance, which is a result from the continuous release of active compounds into the environment for a long period of time.[6–8] Other types of surfaces, which contain copper or silver nanoparticles are those that kill bacteria in contact without continuously releasing biocides.[9–14]

One novel and innovative alternative represents surfaces that catalytically produce bactericides using externally applied chemical, electrical or light energy. To this group belongs light-activated antimicrobial coatings that attract considerable research interest, due to the possibility of continuously disinfect surfaces, overcoming the disadvantages of the other coatings.[5,15] The process is based on the irradiation of photosensitizers with visible light that produces cytotoxic compounds such as singlet oxygen and/or free radicals. It is a similar process as the photodynamic therapy that consists in a treatment of pathogenic cells by the activation of a photosensitizer by light in the presence of oxygen, thus forming highly reactive species (radicals and singlet oxygen) that destroy cells.[16]

Published in : Journal of Applied Polymer Science (2021), vol. 138, n°21, e 50769
DOI: 10.1002/app.50769
Status : Postprint (Author's version)

Currently there are limited number of reports describing the preparation of antibacterial coatings with grafted photosensitizers that act on the principle of photodynamic processes and require oxygen as a third component. A relevant study demonstrated that cellulose acetate coatings loaded with a photosensitizer (toluidine blue) showed almost 94% efficacy against S. aureus and 99.9% against P. aeruginosa upon contact with the impregnated layer under light irradiation at wavelenght of 400–700 nm for 24 h.[17] The combination of two photosensitizers (toluidine blue and bengal rose) in cellulose acetate coatings was also assessed against various grampositive and negative pathogens.[18] Silicon based polymers containing methylene blue also demonstrated antibacterial activity, that was enhanced when combined to gold nanoparticles.[19–20]

Coatings with long lasting activity must present good adhesion to the substrates as well as good chemical and mechanical stability. In recent years, a huge research effort has been devoted to design polymer based coatings that contain catechols as anchoring groups.[21–27] Indeed, catechols have been identified as the main components responsible for the amazing adhesion of mussels, and are present in the so-called mussel adhesive proteins (MAPs) as 3,4-dihydroxy-L-phenylalanine (DOPA) repeating units.[28–33] Many reports were describing the formation of adherent antibacterial coatings based on polymers containing catechol groups. These groups were exploited as anchoring groups to the substrates for long lasting activity, but also for the formation of the biocide in the coating (for instance silver based particles), or the grafting of antibacterial peptides, antibiofilm enzymes or antiadhesion polymers.[34–36] Recently, catechol containing microgels combined with iron magnetic nanoparticle (FeMNP) were designed and were used to generate reactive oxygen species (ROS), thus imparting antimicrobial activity against both E. coli and S. aureus to the microgel.[37]

Here we report the preparation of bio-inspired photoactivate antibacterial coatings on stainless steel. Stainless steel (SS) was used as a substrate in this study since it is widely used in the food industry, in biomedical devices and implants, and in submerged marine structures.[38]

The photoactive antibacterial coatings were based on a quinone-decorated nanogel deposited on a surface precoated by a bio-inspired glue, a cationic polyelectrolyte bearing pendent catechols, and a grafted photosensitizer of the aminoacridine. It is well known that the derivatives of acridine are topical antibacterial and antiparasitic agents[39] which possess strong photobactericidal activity by combination of visible or UV light thus leading to production of cytotoxic reactive oxygen species (ROS) including superoxide radical anion (O_2^-) and singlet oxygen ($_1O_2$).[40]

Published in : Journal of Applied Polymer Science (2021), vol. 138, n°21, e 50769
DOI: 10.1002/app.50769
Status : Postprint (Author's version)

2. Experimental section/ Methods

2.1. MATERIALS

The 9-aminoacridine were purchased from SigmaAldrich and used without further purification. Stainless steel (SS) (304 2R) was provided by ARCELOR-Mittal (Arcelor Research Industry Liege; ARIL). Poly(N-methacryloyl 3,4-dihydroxy-L-phenylalanine methyl ester)-b-poly(2-methacryloxyethyltrimethylammonium chloride) (P(mDOPA)-co-P(DMAEMA+)) copolymer (78% yield, with molar content of DOPA and $DMAEMA^+$ of 13% and 87% respectively determined by ^1H NMR),[21] P(mDOPA)[22] and oxidized (P(mDOPA)/ poly(allylamine) (Pox(mDOPA)/PAH)) cross-linked nanogel (d = 120 nm, PDI = 0.2)[23] were prepared as reported in the mentioned publications.[21–23]

2.2. SYNTHESIS OF AMINO MODIFIED AMINOACRIDINE PHOTOACTIVE COMPOUND

To a solution of 9-aminoacridine (200 mg, 1 mmol) in ethanol (20 ml) was added chloroacetyl chloride (90 µl, 1.1 mmol) dropwise under nitrogen. The mixture was refluxed for 10 h under boiling and hydrazine monohydrate (2 ml, 0.039 mol) was added. Then it was refluxed for 5 h and the precipitated product was collected after filtration and dried at 60C for 24 h under vacuum (Scheme 1).

The synthesized compound 3 showed complex NMR spectra (see ESI, Supporting information, Figure S1) which is typical for the 9-amido acridine derivatives due to their existence in tautomeric equilibrium[41] (Scheme 2).

Scheme 1. Synthesis of amino modified 9-aminoacridine

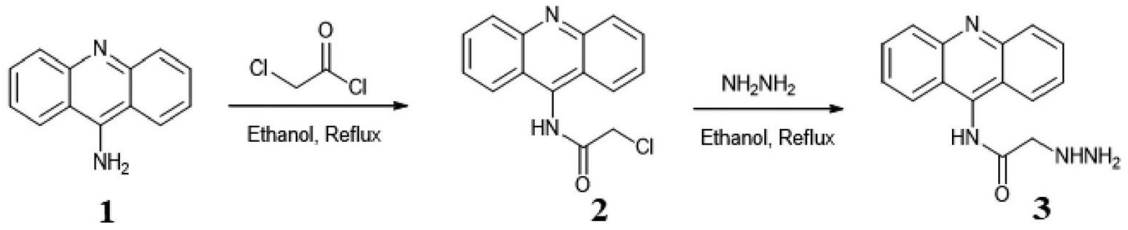

2.3. PREPARATION OF PHOTOACTIVE POLYMER COATINGS ON SS SUBSTRATE

Stainless steel samples with different sizes were cut out from the as-received 1 mm thick SS foils, that is, 2.0 cm × 2.0 cm and 1.0 cm × 1.0 cm for antimicrobial tests. They were cleaned and degreased by twice washing with ethanol and acetone for 5 min respectively. The coating was conducted at

Published in : Journal of Applied Polymer Science (2021), vol. 138, n°21, e 50769
DOI: 10.1002/app.50769
Status : Postprint (Author's version)

room temperature. The substrate was first dipped in an aqueous solution of P(mDOPA)-co-P(DMAEMA$^+$) (2 g L^{-1}, pH 7) for 15 min, then washed twice in deionized water for 5 min, followed by dipping into an aqueous solution of Pox(mDOPA)/ PAH nanogel (1 g L^{-1}) for 15 min and washed with deionized water for 5 min. The final deposition was a solution of 9-aminoacridine 3 (1 g L^{-1}, pH 10), wherein the substrate was dipped for 15 min followed by washing with deionized water for 5 min.

2.4. CHARACTERIZATIONS

2.4.1. QUARTZ CRYSTAL MICROBALANCE COUPLED WITH DISSIPATION

Film growths were followed in real time using quartz crystal microbalance coupled with dissipation (QCM-D) using a Q-Sense E4 equipment. The stainless steel-coated AT-cut resonator (fundamental frequency: 5 MHz) was used as received. First, distilled water was introduced into the cell and the flow was maintained until a stable baseline was obtained. The film deposition started by switching the liquid exposed to the crystal from distilled water to the glue solution P(mDOPA)-co-P(DMAEMA$^+$), (2 g L^{-1} with 0.15 M NaCl) at a flow rate of 200 µl min^{-1}, temperature of 25.09 ± 0.02C. After 15 min, the substrate was rinsed by distilled water to remove the excess of unbounded glue. Then, the deposition of Pox(mDOPA)/PAH nanogels was carried out for 15 min followed by rinsing steps with distilled water. Finally, photoactive 9-aminoacridine 3 solution (1 g L^{-1}, pH 10) was introduced in the system until a stable signal is obtained and further rinsed with distilled water. Sauerbrey equation[42] was used to quantified the amount of the absorbed layers Δm, according to: $\Delta m = \frac{C\Delta f}{-2^n}$, where C is the mass sensitivity constant (17.3 ng cm^{-2} at 4.95 MHz) and n is the overtone number.

Scheme 2. Tautomeric equilibrium of 9-aminoacridine 3

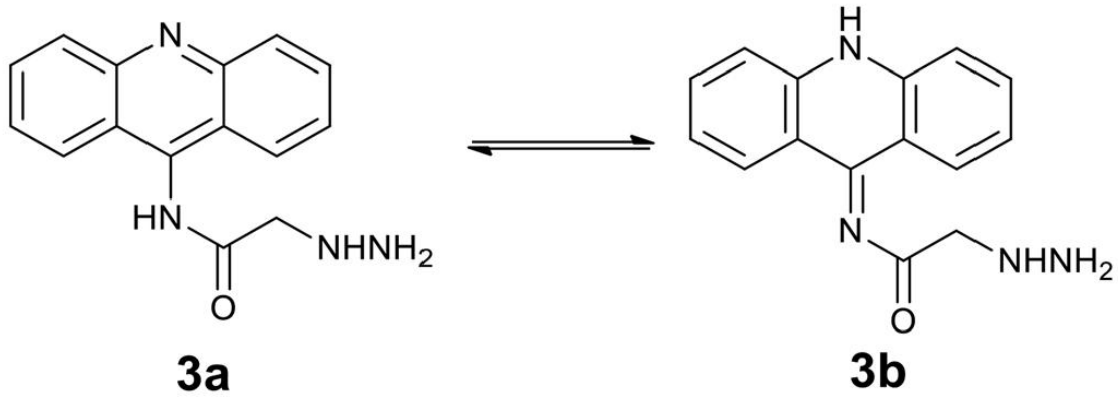

2.4.2. AFM MEASUREMENTS

The surface modifications, resulted from the layer deposition were assessed by image and data acquisitions via Atomic Force Microscopy. The respective images and numeric roughness data were

Published in : Journal of Applied Polymer Science (2021), vol. 138, n°21, e 50769
DOI: 10.1002/app.50769
Status : Postprint (Author's version)

acquired in duplicate for each sample (i.e., from the frontal and back surfaces, respectively). For this purpose, Easyscan-2 by "Nanosurf"- Switzerland, equipped by TAP 190-Al G probes (Budgetsensors, Bulgaria) was used. The image acquisitions were performed on square areas with linear size of 49.5 μm and resolution of 256 points per line for 256 lines, at scanning in dynamic regime at 17 kHz.

2.4.3. SCRATCH TEST WITH SPHERICALCONICAL STYLUS

Scratch testing was performed using UMT (Bruker) scratch test module with a diamond spherical-conical stylus with tip radius (DSH-025, R = 2.5 μm) over a scratch distance of 5 mm with a scratch speed of 0.083 mm/s with gradually increased load from 5 to 50 mN. All scratches were carried out five times in the same direction.

A progressive loading scratch test mode was performed, where the load on the indenter increases linearly as the indenter moves across the test surface at a constant speed and failure was observed. An x-axis slider moves the diamond stylus across the test specimen to produce the scratch. The UMT equipment allows monitoring during the test of the actual normal force, scratching force and coefficient of friction. The scratch line was observed by SEM (Tabletop Hirox SH-4000 M).

2.4.4. NANOINDENTATION MEASUREMENT

Nanomechanical analyses were performed using Universal Nanomechanical Tester (UNMT, Bruker), equipped with Nanoindenter & Atomic Force Microscopy (Ambios Technology). Measurements were made on the SS coated with P(mDOPA)-co-P(DMAEMA^{+})/Pox (mDOPA)/PAN/ 9-aminoacridine 3 layers. For each specimen 48 nanoindentations were made with force applied to 20 mN. The 70 nm diamond tip Berkovich indenter was used to perform the tests and specialized software to calculate the hardness and the modulus of elasticity of the specimens using the Oliver Pharr method.[43] All nanoindentation tests were performed at constant temperature 20C.

2.4.5. PHOTOBACTERICIDAL ACTIVITY

The photobactericidal activity of the photoactived polymer nanogels coated on SS against Gram-negative bacteria Escherichia coli (*E. coli*) was assessed by viable cell-counting method. *E. coli* has been selected as a representative of the best studied species of bacteria which offers a number of advantages in its use in laboratory practice including: ability to grow on relatively cheap chemically defined media, rapid sustainable growth, ability to grow in a wide range of environmental conditions as in the presence and as in the absence of oxygen, harmlessness of the vast majority of laboratory-cultured strains, does not form aggregates, etc.

A preculture of *E. coli* was used to seed a fresh culture into 50 ml nutrient broth LB and the bacterial culture was incubated at 37C for 16 h. The culture contained ca. 10^8 cells.ml^{-1} was used for the test. The original cell concentration was determined by spread plate method. Upon appropriate dilution with sterilized 0.9% saline solution a culture of about 10^6 cells.ml^{-1} was prepared and used for

Published in : Journal of Applied Polymer Science (2021), vol. 138, n°21, e 50769
DOI: 10.1002/app.50769
Status : Postprint (Author's version)

antibacterial testing. Film deposited onto 1x1 cm SS substrate was sterilized using UV-C light disinfection system, 30 W, λ = 254 nm, for 30 min and exposed to the E. coli cell suspension (4 ml containing $7.1.10^5$ CFU.ml^{-1}) using sterile transparent glass bottle (d = 2.5 cm, V = 20 ml). Reactor vessel (glass bottle) was fixed on the surface of dry shaker and illuminated for 19 h using 200 W spotlight (wavelength from 380 nm to 750 nm). At a specified time 0.1 ml of the illuminated cell suspension was added to 0.9 ml sterile 0.9% saline solution and several dilutions are carried out. The surviving bacteria are counted by spread plate method. The similar experiment was performed in dark without illumination of the samples.

3. Results and discussion

3.1. PREPARATION OF THE PHOTOACTIVE POLYMER COATING ON STAINLESS STEEL

The formation of the photoactive polymer coatings was based on a simple process illustrated in Scheme 3. It consists in the sequential deposition of three components in solution in water, (i) a catechol-based cationic glue P(mDOPA)-co-P(DMAEMA$^+$) (2 g L^{-1}), (ii) an orthoquinone functionalized nanogel (Pox(mDOPA)/PAH) (1 g L^{-1}), and (iii) the photosensitizer (amino modified 9-aminoacridine 3) (1 g L^{-1}). P(mDOPA)-co-P (DMAEMA$^+$) containing 13 mol% of DOPA units was used as a universal primer that was reported to facilitate the strong anchoring of antibacterial polymers but also peptides and enzymes to SS.[21–24,44–45] Pox(mDOPA)/PAH nanogels were used to permit the covalent grafting of the photosensitizer by reaction of the amine group of 9-aminoacridine 3 with the quinone group present in the nanogel. Indeed, these nanogels were developed by Detrembleur et all. to covalently graft antibacterial, antibiofilm and antiadhesion peptides/enzymes or polymers on SS by reacting some amine groups of the protein/polymer with o-quinones of the nanogel by Michaël type reaction and/or imine formation.[23] P(mDOPA)-co-P (DMAEMA$^+$)[21] and Pox(mDOPA)/PAH nanogels[23] were prepared according to procedures reported by Detrembleur et all. The chemical modification of 9-aminoacridine was performed according to Scheme 1. The hydrazino modified 9-aminoacridine (compound 3) was synthesized according to a two steps process by using chloroacetyl chloride to form the intermediate compound 2 that was then modified by hydrazine monohydrate to provide the final product.

The photoactive coating was thus achieved by simply dipping the SS substrate into the different solutions, with a rinsing step with water before each deposition to remove excess of unbound polymer or nanogel (Scheme 3).

Published in : Journal of Applied Polymer Science (2021), vol. 138, n°21, e 50769
DOI: 10.1002/app.50769
Status : Postprint (Author's version)

The deposition of all layers and formation of photoactive polymer coating on SS was followed by using QCM-D in real time on SS sensors by measuring the variation of the resonant frequency (Df) vs. time (Figure 1). This technique already demonstrated to be robust to follow on-line the deposition of products on various substrates, and to evaluate whether the coating remained on the surface after rinsing with a good solvent of the coating. A decrease in Df indicates polymer deposition.[46] An aqueous solution of the biomimetic glue, P(mDOPA)-coP(DMAEMA$^+$) (2 g L^{-1}), was flowed through the cell at room temperature, and the sharp decrease in frequency testified for the deposition of the copolymer that remained on the substrate even after rinsing with water with calculated amount of deposited copolymer Δm_1 = 23 ng cm^{-2}, according to Sauerbrey equation. The next step was the deposition of the second Pox(mDOPA)/ PAH nanogel. The nanogel deposition was slower, however the more important drop in frequency indicated a high content of product deposited with calculated amount of Δm_2 = 63 ng cm^{-2}. Rinsing with water removed excess of unbound nanogel. The last step was the deposition of the photoactive dye solution based on 9-aminoacridine 3, which was confirmed after its rinsing with water. The amount of the last photoactive layer was calculated to be Δm_3 = 69.1 ng cm^{-2}, which is indicative for the high content of deposition of the last photoactive layer. This QCM-D experiment therefore showed that the three products were successfully deposited on SS and remained on the substrate even after rinsing with water.

The surface topography is known to affect bacterial attachment and subsequent biofilm formation.[47] Therefore, the surface roughness was assessed by atomic force microscopy (AFM) by evaluating the arithmetical average height, R_a[48–49] of four different surfaces Figure 2: (a) pristine SS (Figure 2(a)) and SS modified by (b) P(mDOPA)-co-P(DMAEMA$^+$) (Figure 2(b)), (c) P(mDOPA)-co-P(DMAEMA$^+$)/Pox(mDOPA)/PAH nanogel (Figure 2(c)), (d) P(mDOPA)-co-P(DMAEMA$^+$)/Pox (mDOPA)/PAH/photosensitizer 3 (Figure 2(d)). The data showed that pristine SS was very rough with a R_a value of 347 nm with the highest deviation between two points. This Ra value slightly decreased by the increment of the deposited layer thickness, as expected, to 342 nm for the first P(mDOPA)-co-P(DMAEMA$^+$) layer to 302 nm with the second layer of Pox(mDOPA)/PAH nanogel, and finally to 284 nm with the photosensitizer. However, these differences are quite low because the coatings are expected to be thin and were therefore deposited epitaxially by repeating the relief of the quite rough pristine SS substrate. The comparable roughness of the different surfaces reflected their capability to follow the morphology of the substrate.

Published in : Journal of Applied Polymer Science (2021), vol. 138, n°21, e 50769
DOI: 10.1002/app.50769
Status : Postprint (Author's version)

Scheme 3. Procedure for the formation of photoactive polymer coating on stainless steel substrate [Color figure can be viewed at wileyonlinelibrary.com]

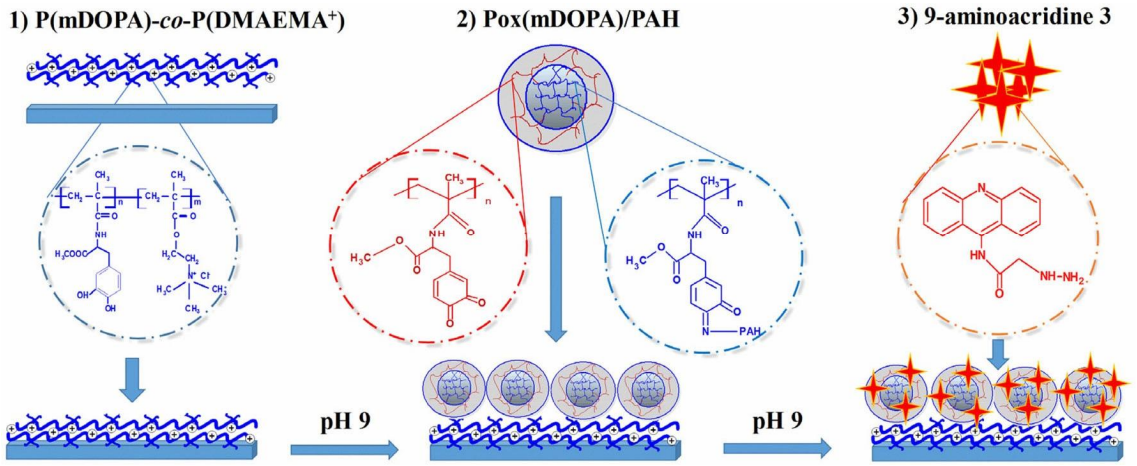

Figure 1. Frequency change upon deposition of P(mDOPA)co-P(DMAEMA⁺), Pox(mDOPA)/PAH nanogel and 9-aminoacridine 3 dye measured by QCM-D as a function of time at 25° C, where the overtone number is 7

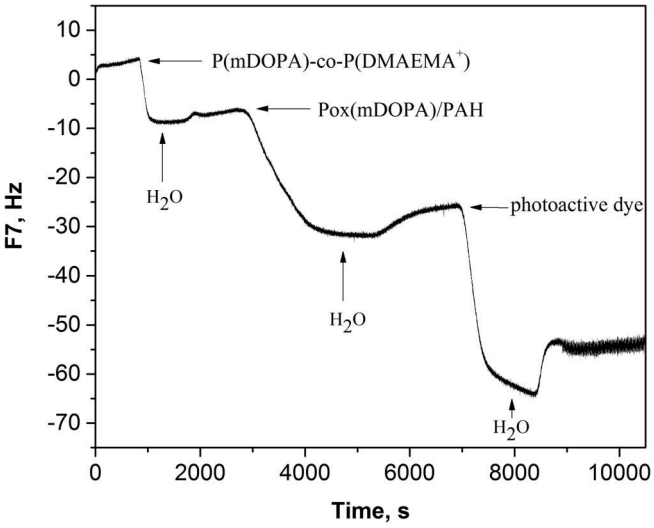

Published in : Journal of Applied Polymer Science (2021), vol. 138, n°21, e 50769
DOI: 10.1002/app.50769
Status : Postprint (Author's version)

Figure 2. 3D topology of the coatings obtained by AFM: (a) pristine SS; (b) P(mDOPA)-co-P(DMAEMA+) copolymer; (c) P(mDOPA)co-P(DMAEMA+)/Pox(mDOPA)/PAH; (d) P(mDOPA)-co-P(DMAEMA+)/Pox(mDOPA)/PAH/photosensitizer [Color figure can be viewed atwileyonlinelibrary.com]

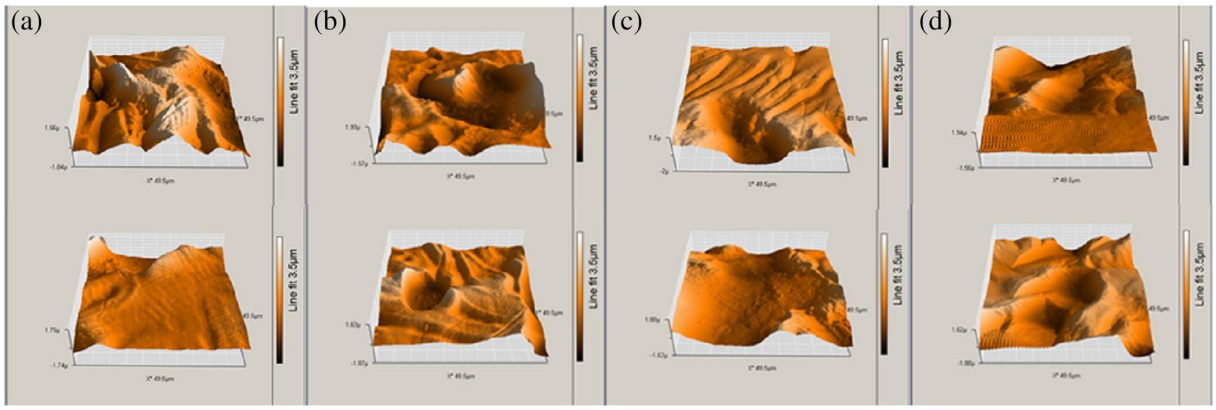

3.2. NANOMECHANICAL PROPERTIES OF POLYMER COATINGS ON SS

3.2.1. SCRATCH TESTING

Scratch testing is one of the most widely used and popular approach in the assessment of the adhesion strength of a coating-substrate system. In this method, a hard diamond or metal spherical-tipped indenter with a typical radius of 200 μm is used to apply an increasing load on the surface of the coating continuously. At the same time, the sample is displaced at a constant velocity. Scratching of the surface results in an increase in elastic and plastic deformation until extensive spalling of the coating from the substrate occurs at a critical load. The critical load is generally determined using optical microscopy, acoustic emission, or friction force measurements. In the present study, the scratch test was performed on the SS substrate coated with P(mDOPA)-co-P(DMAEMA$^+$)/Pox (mDOPA)/PAH/photosensitizer layers applying gradually increased load from 5 to 50 mN. Figure 3 shows the typical average load (N) range at which the coating failed during scratch testing.

The scratching process is accompanied by the emission of acoustic signals which are small when the film adheres at low loads until 15 mN. The increasing of the acoustic signals was observed at a displacement force of 15 mN, which is indicative for the beginning of the scratching of the deposited polymer coatings on SS. The coefficient of friction (COF) is relatively constant with an average value of 0.75 at standard deviation of 0.18, assuming that the polymer coating possessed a uniform thickness (Figure 3). SEM images (Figure 4) demonstrated a linear increasing scratch track on the photoactive polymer nanogel coatings formed on SS substrate under loading from 5 to 50 mN (Figure 4(a)-(c)). As seen, no cracking nor delamination of the coatings during the scratch was observed. The increasing of normal load from 15 mN to 50 mN leads to slight expansion of the

Published in : Journal of Applied Polymer Science (2021), vol. 138, n°21, e 50769
DOI: 10.1002/app.50769
Status : Postprint (Author's version)

scratch track with formation of small amount of debris along the track sides (Figure 4(d)-(f)). The relatively small amount of debris from the scratching and lack of peeling of the film can suggest a good scratch resistance and adhesive strength of the coatings on SS.

Figure 3. Scratch test on SS substrate coated with P(mDOPA)-co-P(DMAEMA+)/Pox(mDOPA)/PAH/photosensitizer layers; Fz – Normal force (mN), AE - acoustic emission (volt) and COF - coefficient of friction. The inset shows the SEM image of the corresponding scratch track [Color figure can be viewed at wileyonlinelibrary.com]

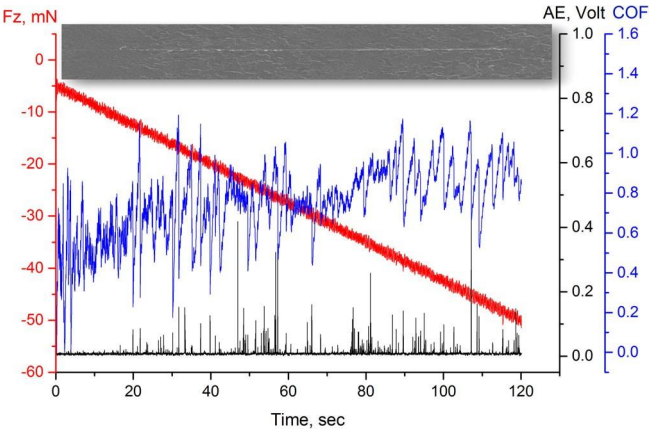

Figure 4. SEM images of the scratch track under loading from 5 to 50 mN

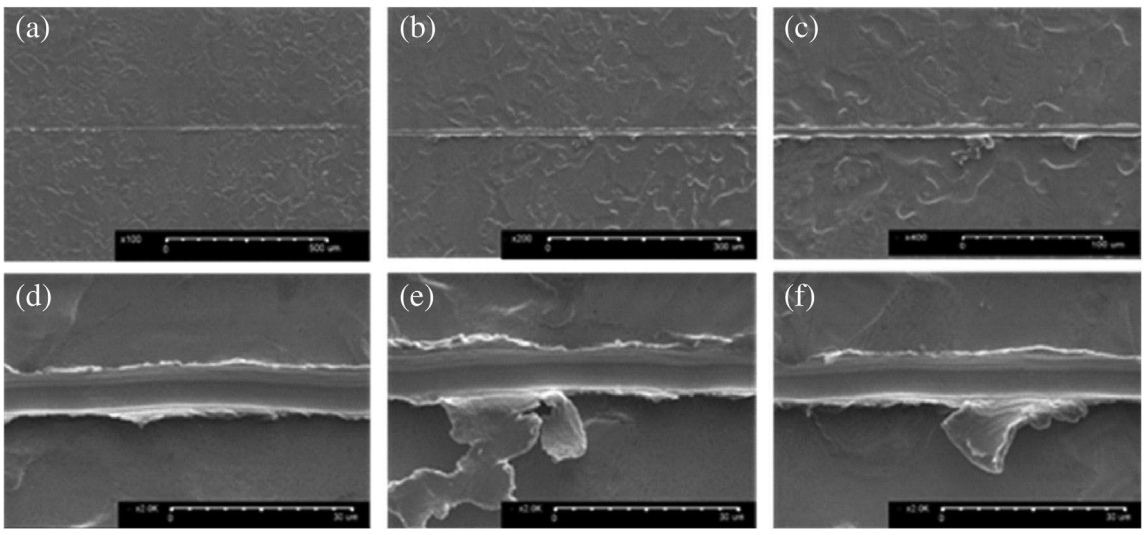

3.2.2. NANOINDENTATION MEASUREMENT OF PHOTOACTIVATE POLYMER COATINGS

Nanoindentation, also named depth-sensing indentation or instrumented indentation, is based on the theories of contact mechanics. The test provides information on elastic modulus, hardness, strain-hardening, cracking, phase transformations, creep, and energy absorption.[50] This technique

Published in : Journal of Applied Polymer Science (2021), vol. 138, n°21, e 50769
DOI: 10.1002/app.50769
Status : Postprint (Author's version)

is widely used in the characterization of mechanical properties of thin films, coatings, and other nanomaterials.

In this study, the photoactive polymer coatings deposited on a SS substrate was subjected to the nanoindentation measurement using Berkovich nanohead at a maximum load of 20 mN (Figure 5). Example load–displacement curves at maximum load of 20 mN obtained from 48 nanoindentations of the photoactive polymer coatings on SS are presented in Figure 5(a). Using experimental results, Olive Pharr model is applied for calculating the nanomechanical characteristics, such as hardness, Young's modulus of elasticity and contact stiffness[43] and the results are presented in Figure 5(b). The surface elastic modulus was calculated from the stiffness of the contact during initial unloading in conjunction with the contact area. Indentation hardness is also the mean stress or pressure in an indentation experiment, that is, it is the ratio of force, P, to contact area, A, where A is in generally related to displacement, h, by the tip geometry.

The relatively narrow hysteresis of the load– displacement curves indicates a relatively uniform polymer film thickness on the substrate. A maximum Young's modulus of 0.6 GPa and hardness of 0.21 GPa were determined from the nanoindentation measurements of the photoactive polymer coating.

The decrease of these values with increasing depth of penetration of the indenter (Figure 5b) can be associated with the linear viscoelasticity of the polymer film, which in depth is the reason for the slower relaxation of the applied normal stress.

3.3. ANTIBACTERIAL PHOTOACTIVITY

The antibacterial photoactivity of the coatings was determined against Gram-negative *E. coli* strain. The preliminary results of the performed antibacterial photoactivity tests of thus obtained photoactive polymer coatings on SS determined by viable cell-counting method under illumination using 200 W spotlight (wavelength from 380 nm to 750 nm) showed that after 2 h of contact the reducing rate increase to 87.4% and after 18 h of contact the reducing rate of 100% was determined (Table 1).

When the coating was not illuminated, a weaker antibacterial activity of the coatings was observed at the 1 h and 2 h of contact in comparison to the illuminated photoactive polymer coating, however after 18 h of contact the reducting rate was 100% as well. This results suggest that the antibactericidal activity of the coatings is a result of the combined effect on the photodynamic activity of the coating and on its antibacterial activity due to an alternative mechanism of action. We thus conclude that for the precise quantitative determination of photobacterial activity of the obtained coatings, in future it is necessary to use another laboratory system, allowing physical separation of microorganisms from the photoactive surface.

Published in : Journal of Applied Polymer Science (2021), vol. 138, n°21, e 50769
DOI: 10.1002/app.50769
Status : Postprint (Author's version)

Figure 5. (a) Load–displacement curves of 48 nanoindentations and (b) hardness and Young's modulus as a function of contact depth on photoactive polymer nanogel coatings on SS [Color figure can be viewed at wileyonlinelibrary.com]

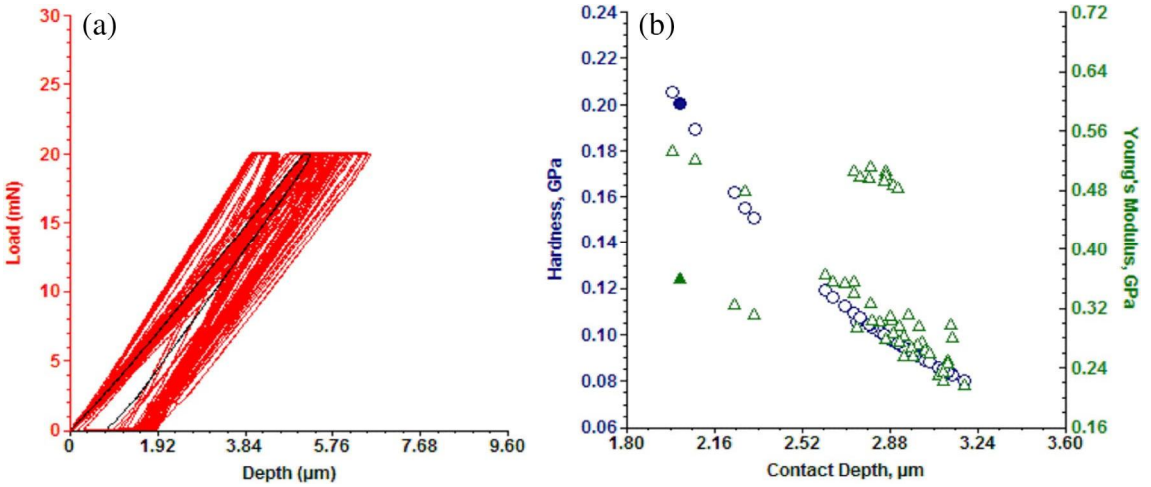

Table 1. Antibacterial photoactivity of photoactive polymer nanogel coatings on SS substrate against E. coli (T0 = 7.1.105 CFU.Ml 1 T0 - Initial number of bacteria per ml used for the test)

	1 h of contact		2 h of contact		18 h of contact	
Sample	Survived cells, CFU.ml^{-1}	Reduction rate, [%]	Survived cells, CFU.ml^{-1}	Reduction rate, [%]	Survived cells, CFU.ml^{-1}	Reduction rate, [%]
photoactive polymer coating on SS with illumination	5.1x10^5	28.2	8.9x10^4	87.4	0	100
photoactive polymer coating on SS without illumination	6.25x10^5	12.0	3.3x10^5	53.5	0	100

4. Conclusion

In this work, we have prepared a novel environmental friendly and reactive photoactive polymer coatings on stainless steel and assessed its antibacterial activity under visible light irradiation. This was achieved using reactive quinone decorated nanogels on stainless steel pre-coated by a biomimetic glue, followed by the covalent grafting of a photosensitizer of the 9-aminoacridine-3 type. All deposition steps were facile using aqueous based solutions, and the formation of the polymer coatings was demonstrated by using QCM-D measurements. The surface properties of the thin coating were investigated applying AFM analysis and this technique also evidenced that the coatings was repeating the relief of the rough pristine SS substrate. The mechanical properties of

Published in : Journal of Applied Polymer Science (2021), vol. 138, n°21, e 50769
DOI: 10.1002/app.50769
Status : Postprint (Author's version)

thus prepared coatings using an innovative nanoindentation technique showed good hardness and Young's modulus. Finally, the preliminary investigation of the antibacterial photoactivity against Gram-negative *E. coli* demonstrated that the photoactive polymer coatings possess strong antibacterial activity and can be used as a platform for the preparation of antibacterial polymer coatings for medical applications.

ACKNOWLEDGMENTS

The authors gratefully acknowledge the financial support from the National Science Fund of Bulgaria (project no. KP-06-H29/5). Christophe Detrembleur is Research Director by F.R.S.- FNRS.

CONFLICT OF INTEREST

The authors declare no conflict of interest.

ORCID

RAYNA BRYASKOVA HTTPS://ORCID.ORG/0000-0002-2096-7257

SUPPORTING INFORMATION

Additional supporting information may be found online in the Supporting Information section at the end of this article.

HOW TO CITE THIS ARTICLE:

Bryaskova R, Philipova N, Georgiev N, Lalov I, Bojinov V, Detrembleur C. Photoactive mussels inspired polymer coatings: Preparation and antibacterial activity. J Appl Polym Sci. 2021;e50769. https://doi.org/10.1002/app.50769

Published in : Journal of Applied Polymer Science (2021), vol. 138, n°21, e 50769
DOI: 10.1002/app.50769
Status : Postprint (Author's version)

References

[1] W. A. Rutala, D. J. Weber, Infect. Control Hosp. Epidemiol. 2011, 32, 743.

[2] A. Davies, T. Pottage, A. Bennett, J. Walker, J. Hosp. Infect.2011, 77, 199.

[3] J. A. Otter, S. Yezli, J. Hosp. Infect. 2011, 77, 83.

[4] X. Zhang, L. Wang, L. Erkki, RSC Adv. 2013, 30, 12003.

[5] D. J. Weber, W. A. Rutala, Am. J. Infect. Control. 2013, 41, S31.

[6] J.-Y. Maillard, Clin. Risk Manag. 2005, 1, 307.

[7] D. J. Weber, W. A. Rutala, Infect. Control. Hosp. Epidemiol.2006, 27, 1107.

[8] W. A. Rutala, D. J. Weber, Emerg. Infect. Dis. 2001, 7, 348.

[9] C. Shuai, Y. Xu, P. Feng, G. Wang, S. Xiong, S. Peng, Chem. Eng. J. 2019, 374, 304.

[10] A. El-Fahama, A. M. Atta, S. M. Osman, A. O. Ezzat, A. M. Elsaeed, Z. A. A. L. Othman, H. A. Al-Lohedan, Prog. Org. Coat. 2018, 123, 209.

[11] H. F. G. Mejía, L. Yohai, A. Pedetta, K. H. Seitz, R. A. Procaccini, S. A. Pellice, J. Colloid Interf, Sci. 2017, 508, 332.

[12] J. Elguindi, X. Hao, Y. Lin, H. A. Alwathnani, G. Wei, C. Rensing, Appl. Microbiol. Biotechnol. 2011, 91, 237.

[13] D. Mitra, M. Li, E. T. Kang, K. G. Neoh, ACS Appl. Mater. Interfaces 2019, 11, 73.

[14] D. Mitra, E. T. Kang, K. G. Neoh, ACS Appl. Mater. Interfaces 2020, 12, 21159.

[15] G. B. Hwang, H. Huang, G. Wu, et al., Nat. Commun. 2020, 11, 1207. https://doi.org/10.1038/s41467-020-15004-6.

[16] L. Benov, Med. Princ. Pract. 2015, 24, 14.

[17] K. S. Soni, S. S. Desale, T. K. Bronich, J. Controll. Release. 2016, 240, 109.

[18] M. Wilson, Infect. Control Hosp. Epidemiol. 2003, 24, 782.

[19] V. Decraene, J. Pratten, M. Wilson, Appl. Environ. Microbiol. 2006, 72, 4436.

[20] S. Ismail, S. Perni, J. Pratten, I. Parkin, M. Wilson, Infect. Control. Hosp. Epidemiol. 2011, 32, 1130.

[21] A. Charlot, V. Sciannamea, S. Lenoir, E. Faure, R. Jérôme, C. Jérôme, C. Van de Weerdt, J. Martial, C. Archambeau, N. Willet, A.-S. Duwez, C.-A. Fustin, C. Detrembleur, J. Mater. Chem. 2009, 19, 4117.

[22] E. Faure, P. Lecomte, S. Lenoir, C. Vreuls, C. Van De Weerdt, C. Archambeau, J. Martial, C. Jerome, A.-S. Duwez, C. Detrembleur, J. Mater. Chem. 2011, 21, 7917.

Published in : Journal of Applied Polymer Science (2021), vol. 138, n°21, e 50769
DOI: 10.1002/app.50769
Status : Postprint (Author's version)

[23] E. Faure, C. Falentin, T. S. Lanero, C. Vreuls, G. Zocchi, C. Van de Weerdt, J. Martial, C. Jérôme, A.-S. Duwez, C. Detrembleur, Adv. Funct. Mater. 2012, 22(24), 5271.

[24] E. Faure, C. Falentin-Daudré, C. Jérôme, J. Lyskawa, D. Fournier, P. Woisel, C. Detrembleur, Prog. Polym. Sci. 2013, 38 (1), 236.

[25] J. Horsch, P. Wilke, M. Pretzler, M. Seuss, I. Melnyk, D. Remmler, A. Fery, A. Rompel, H. G. Börner, Angew. Chem. Int. Ed. Engl. 2018, 57(48), 15728.

[26] J. Saiz-Poseu, J. Mancebo-Aracil, F. Nador, F. Busqué, D. Ruiz-Molina, Angew. Chem. Int. Ed. Engl. 2019, 58(3), 696.

[27] A. H. Hofman, I. A. van Hees, J. Yang, M. Kamperman, Adv. Mater. 2018, 30(19), e1704640.

[28] J. H. Waite, M. L. Tanzer, Science 1981, 212, 1038.

[29] H. Lee, S. M. Dellatore, W. M. Miller, P. B. Messersmith, Science 2007, 318, 426.

[30] N. Patil, C. Jérôme, C. Detrembleur, Prog. Polym. Sci. 2018, 82, 34.

[31] J. Sedó, J. S. Poseu, F. Busqué, D. R. Molina, Adv. Mater. 2013, 25, 653.

[32] Q. Lyu, N. Hsueh, C. L. L. Chai, ACS Biomater. Sci. Eng. 2019, 5(6), 2708.

[33] B. P. Lee, H. Birkedal, H. Lee, Front. Chem. 2019, 7, 883.

[34] A. Chiloeches, C. Echeverría, R. C. Rodríguez, D. Plachà, F. L. Fabal, M. F. García, A. M. Bonilla, Progr. Org. Coat. 2019, 136, 105272.

[35] M. M. Couranjou, R. Mauchauffé, S. Bonot, C. Detrembleur, P. Choquet, J. Mat. Chem. B. 2018, 6(4), 614.

[36] Y. E. Cheng, J. Y. Zhang, Y. B. Wang, C. M. Li, Z. S. Lu, X. F. Hu, L. Q. Xu, Mater. Sci. Eng. C. 2019, 98, 649.

[37] Z. Zhang, X. He, C. Zhou, M. Reaume, M. Wu, B. Liu, B. P. Lee, ACS Appl. Mater. Interfaces. 2020, 12(19), 21210.

[38] L. Q. Xu, D. Pranantyo, K.-G. Neoh, E. T. Kang, S. L.-M. Teo, G. D. Fu, Polym. Chem. 2016, 7, 493.

[39] M. Wainwrighta, D. A. Phoenix, J. Marland, D. R. A. Wareing, F. J. Bolton, J. Antimicrob. Chemother. 1997, 40, 587.

[40] M. Wainwright, J. Antimicrob. Chemother. 2001, 47, 1.

[41] Borovlev, O. Demidov, G. Amangasieva, E. Avakyan, Tetrahedron Lett. 2016, 57, 3608.

[42] G. Z. Sauerbrey, Phys. 1959, 155, 206.

[43] W. C. Oliver, G. M. Pharr, J. Mater. Res. 2004, 19, 3.

[44] C. Vreuls, G. Zocchi, H. Vandegaart, E. Faure, C. Detrembleur, A.-S. Duwez, J. Martial, C. Van De Weerdt, Biofouling 2012, 28(4), 395.

Published in : Journal of Applied Polymer Science (2021), vol. 138, n°21, e 50769
DOI: 10.1002/app.50769
Status : Postprint (Author's version)

[45] C. Faure, C. Vreuls, C. F. Daudré, G. Zocchi, C. Van de Weerdt, J. Martial, C. Jérôme, A.-S. Duwez, C. Detrembleur, Biofouling 2012, 28(7), 719.

[46] K. A. Marx, Biomacromolecules 2003, 4, 1099.

[47] R. S. Friedlander, H. Vlamakis, P. Kim, M. Khan, R. Kolter, J. Aizenberg, Proc. Natl. Acad. Sci. U. S. A. 2013, 110, 1.

[48] Whitehead, J. Verran, Food Bioprod. Process 2006, 84, 253.

[49] R. J. Crawford, H. K. Webb, V. K. Truong, J. Hasan, E. P. Ivanova, Adv. Colloid Interface Sci. 2012, 17, 142.

[50] A. C. Fischer-Cripps, D. W. Nicholson, Appl. Mech. Rev. 2004, 57, B12.